Int. J. Nanosci. Nanotechnol., Vol. 13, No. 3, Month. 2017, pp. 227-239

Modeling and Simulation of Spherical and Cylindrical Contact Theories for Using in the Biological Nanoparticles Manipulation

M. Habibnejad Korayem*, R. N. Hefzabad and M. Taheri

Robotic Research Laboratory, Center of Excellence in Experimental Solid Mechanics and Dynamics, School of Mechanical Engineering, Iran University of Science and Technology, P.O.Box 16846-13114, Tehran, Iran.

(*) Corresponding author: hkorayem@iust.ac.ir
(Received: 24 May 2016 and Accepted: 26 September 2016)

Abstract

The low Young's modulus of biological particles results in their large deformation against the AFM probe forces; therefore, it is necessary to study the contact mechanics of bioparticles in order to predict their mechanical behaviors. This paper specifically deals with the contact mechanics of DNA nanoparticles with spherical and cylindrical shapes during manipulation. In previous studies, these nanoparticles have been investigated in the elastic regime, which is not appropriate for biological particles. Therefore, in this paper, elastoplastic contact has been studied and compared with the other existing models. The contact regions have been analyzed by Hertz, JKR and Chang models for spherical contact and by Hertz and JKR models for cylindrical contact and compared with the FEM results. The results of this article indicate that JKR model is slightly different from the elastic simulation and that for the same magnitude of applied force, the elastoplastic models show a larger deformation for DNA nanoparticles relative to the elastic case.

Keywords: *Nanomanipulation, Contact mechanics models, Elastoplastic contact, DNA, FEM*.

Nomenclature	
a	contact radius
A	contact area
A_C	critical contact area
E_1	Young's modulus of first body
E_2	Young's modulus of second body
F	external force
$F_{(adh)}$	adhesion force
F_C	critical force
k	reduced modulus of elasticity
L	length of cylindrical body
R	effective radius
R_1	radius of first body
R_2	radius of second body
γ	surface energy
γ_1	surface energy of first body
γ_2	surface energy of second body
γ_{12}	interfacial energy
δ	normal indentation depth
δ_C	critical indentation depth
v	Poisson's ratio
v_1	Poisson's ratio of first body
v_2	Poisson's ratio of second body

1. INTRODUCTION

Atomic force microscopy has been developed for topography in micro and nano scales, and it is very useful for high-precision imaging of bio-samples such as cells, proteins and DNA [1]. Numerous research works have been performed on the subject of nanomanipulation and its applications. The study of nanomanipulation systems by Sitti can be mentioned as one of these activities [2]. By using the spherical contact theory of JKR, Sitti and Tafazzoli presented dynamic behavior of particle during AFM-based nanomanipulation [3]. Korayem and Zakeri performed sensitivity analyses of critical parameters in AFM-based nanomanipulation, which included the critical force and time of nanoparticles pushing versus the changes of all the parameters of the nanomanipulation process. Korayem et al. also conducted the sensitivity analysis of different frictional

models in the manipulation of nanoparticles. [4]. Subsequently, Korayem et al. investigated JKR contact model in biomanipulation. They ultimately compared their results with the results obtained from the gold nanoparticles under similar conditions and with the theoretical and experimental results obtained from the embryonic cells of mice. They indicated that different forces are needed to produce the same deformation in DNA and gold nanoparticles, which is due to the difference in the Young's modulus of these particles. This claim was also verified by sensitivity analysis [5]. In the other work, Korayem et al. investigated the effect of nanoparticle geometry and material [6].

Molecular dynamics method is one of the approaches that are used for studying manipulation of biological samples. These methods are usable in small scale physical processes [7]. Firouzi et al. used the molecular dynamics simulation to investigate the manipulation process when a nanoprobe tries to move a bio-sample on a substrate [8].

In the last decades, the scientists have become interested in studying the biological cells and in estimating their mechanical properties and the effect of various parameters on these properties [9]. Dimitriadis et al. investigated the limitations of the use of the widely available AFM cantilevers with the sharp tips but poorly defined tip geometry; further develop the use of microspheres as indenters [10]. Mechanical properties such as elasticity, membrane tension, cell shape, and adhesion resistance play important roles in the proliferation of these cells. The mechanical characteristics of biological cells have been examined by different means. The optical tweezers, magnetic beads and micropipette aspiration are the most common of these methods. However, these techniques cannot provide the accuracy which is afforded by the atomic force microscopy [11]. Hence, an investigative branch of contact mechanics is needed in research works performed by this instrument. Briscoe et al. described various analytical procedures that account for the influence of the geometry of a rigid indenter upon the measured contact compliance of a smooth perfectly elastic hall space [12].

As finite element methods develop in biology, in recent years, behavior of biologic materials are studied using these methods.

The influences of geometrical parameters on the measured values using micro-indentation have been examined by Bolduc et al.; they studied the effects of geometrical variables such as cell radius, cell wall thickness, and tip radius [13]. Finite element simulation of viral capsid nanoindentation was executed by Gibbons and Klug. They used ABAQUS finite element software package for their analysis [14]. Indentation of three prostate cancer cells which have low elasticity modulus and are considered ductile materials was conducted using Hertz contact mechanics model and validated by FEM [15]. Korayem and Rastgar modeled small deformation of biological cell based on contact models and compared with FEM [16].

In this paper, first, the spherical contact models of Hertz and JKR have been explored for the elastic contact and the Chang model has been investigated for the elastoplastic DNA nanoparticle-tip contact and then, to get closer to the geometry of the real particle, the cylindrical contact mechanics models of Hertz and JKR have been considered. Next, the DNA particle has been investigated as the target particle, and its contact mechanics has been simulated by means of the abovementioned contact models. To compare the results, a FEM simulation of DNA nanoparticle has been done and the simulation results of the contact models have been compared with those of the finite element method.

2. MATERIAL

The deoxyribonucleic acid, or DNA, is a nucleic acid molecule that contains the

genetic structures and plays a role in the development and functioning of all the known live organisms. The components of DNA that carry this genetic information are called genes. The other strands of DNA have structural functions or they are involved in regulating the use of genetic information. This cell together with the RNA and proteins form the three main macromolecules that are essential for all life forms. DNA is made of two long polymer strands containing simple units called nucleotides, which are connected to one another by ester bonds on backbones consisting of sugars and phosphates. These two strands wind in opposite directions; hence they are unparallel to each other. To each sugar base, one of the four molecules called nucleobases is attached. The order in which these four nucleobases are arranged on the backbone determines how genetic information is coded. This information is read by a genetic code and, thus, the order of amino acids within proteins is determined [17].

The studies show that in investigating the behavior of the DNA molecule during contact, the strands of this particle can be considered as a spherical pack [18-20]. Fig. 1(a) illustrates such a geometrical configuration. In studies on the mechanics of DNA packaging, Purohit et al. used the theory of elasticity and a simple model of load and hydration forces to measure the needed force for the packaging of DNA in a capsid. In their examination, three simplified models of virus capsids were presented for measuring the packaging energy [21,22]. In another work which investigates the bending elasticity of DNA and the effects of liquid viscosity and capsid expansion during the packaging process, they presented three models of ideal geometries and also the dimensions of some viruses [23]. Fig. 1(b) shows a representation of the abovementioned description.

3. THEORY

During the process of nanomanipulation by an AFM, the exerted forces on the

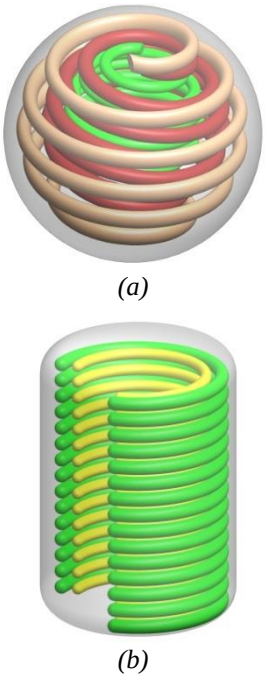

(a)

(b)

Figure 1. *Packing of DNA molecule: (a) Circular DNA, (b) Cylindrical DNA.*

contact region cause the indentations in the nanoparticle and tip/substrate, which are considerable in nano scale and affect the nanomanipulation process. The characteristics of the contact region are obtained by the theories of contact mechanics. This section deals with the modeling of the used contact theories. First, the equations in which the targeted nanoparticle has been considered as a sphere are described and then the equations are developed for cylindrical nanoparticles are expressed.

3.1. Spherical Contact Mechanics Models

3.1.1. Hertz Contact Theory

A very famous model for the contact between two spheres was developed by Hertz [24]. His assumptions for solving this contact problem were as follows: 1) The contact region is elliptical, 2) Each body is considered as an elastic half-space, 3) The dimensions of the contact area should be small in comparison with the dimensions of each body and the curvature radius, 4) For the linear elasticity to be valid, the strains should be sufficiently small, and 5) The contact is frictionless;

thus, only the normal force is transferred [24].
The normal indentation and contact radius can be extracted from the equations (1-3) by having the externally applied force:

$$F_{(adh)Hertz} = 0 \quad (1)$$

$$\delta_{Hertz} = \frac{a_{Hertz}^2}{R} \quad (2)$$

$$a_{Hertz} = \sqrt[3]{\frac{R}{k}F} \quad (3)$$

In the above equations, the effective radius of the two contacting surfaces with radiuses R_1 and R_2 is $R = R_1R_2/(R_1+R_2)$, and k is the reduced modulus of elasticity, which is obtained from the equation (4):

$$\frac{1}{k} = \frac{m}{2}\left(\frac{1-\nu_1^2}{E_1} + \frac{1-\nu_2^2}{E_2}\right) \quad (4)$$

where m is a constant parameter whose depends on the probe geometry ($m = 1$ for cylindrical tips, $m = 1.5$ for spherical tips and $m = 2$ for conical shapes). In the modeling of contact between the AFM tip and biological cells, the geometry of nanoparticle has been assumed as spherical and the equations of contact between two spheres have been used for this simulation.

3.1.2- JKR Contact Theory

In the absence of adhesion, Hertz model describes the contact surfaces based on elastic contact. One of the contact models that incorporate the surface attraction forces is the JKR contact model. Having the magnitude of the externally applied force and the surface energy, the values of normal indentation depth, contact radius can be obtained from the equations (5-7) [25]:

$$F_{(adh)JKR} = -\frac{3}{2}\pi\gamma R \quad (5)$$

$$\delta_{JkR} = \frac{a_{JkR}^2}{R} - \sqrt{\frac{8\pi\gamma a_{JKR}}{3k}} \quad (6)$$

$$a_{JKR} = \left[\frac{R}{k}\sqrt{F_{(adh)JKR}} + \sqrt{F - F_{(adh)JKR}}\right]^{1/3} \quad (7)$$

In JKR contact model, the surface energy is half of the adhesion energy ($\gamma = \gamma_1 + \gamma_2 - \gamma_{12}$).

3.1.3. Chang Contact Theory

For contacts with small deformations (contact strain of $\delta/R < \%1$), Hertz theory well describes the force-displacement relationships, but this theory cannot describe contacts with large deformations. Tatara realized that the limitations of the Hertz's solution can be removed to some extent by considering the effects of the forces exerted by the opposing sphere. He offered an implicit solution that describes the behavior of elastic spheres in contacts with large deformations ($\delta/R < \%20$). The indentation depth and contact radius in this model can be determined by the equations (8 & 9), where E is the elasticity modulus of the target particle.

$$a_{Tatara} = \sqrt[3]{\frac{3(1-\nu^2)RF}{4E}} \quad (8)$$

$$\delta_{Tatara} = \frac{F}{ka_{Tatara}} - \frac{F}{\pi E}\left[\frac{1-\nu^2}{\sqrt{a_{Tatara}^2 + 4R^2}} + \frac{2(1+\nu)R^2}{(a_{Tatara}^2 + 4R^2)^{3/2}}\right] \quad (9)$$

In studying the elastoplastic contact of rough surfaces, Chang et al. employed a contact model for materials with work hardening [26]. In this model, contact is in the elastic range when $\delta/\delta_C < 1$. δ_C is the critical indentation depth and it is proportional to the critical load which leads to the onset of yield.

$$F_{Chang} = kR^{1/2}\delta_{Chang}^{3/2} = F_C\left(\frac{\delta_{Chang}}{\delta_C}\right)^{3/2} \quad (10)$$

when $\delta_{Chang}/\delta_C > 1$, the contact is completely elastoplastic and these

equations should be numerically solved for the sphere.

$$\begin{aligned}
&\frac{F_{Chang}}{F_C}=1.03\left(\frac{\delta_{Chang}}{\delta_C}\right)^{1.425},1\le\frac{\delta}{\delta_C}\le 6\\
&\frac{A_{Chang}}{A_C}=.93\left(\frac{\delta_{Chang}}{\delta_C}\right)^{1.136},1\le\frac{\delta}{\delta_C}\le 6\\
&\frac{F_{Chang}}{F_C}=1.4\left(\frac{\delta_{Chang}}{\delta_C}\right)^{1.236},6\le\frac{\delta}{\delta_C}\le 110\\
&\frac{A_{Chang}}{A_C}=.94\left(\frac{\delta_{Chang}}{\delta_C}\right)^{1.146},6\le\frac{\delta}{\delta_C}\le 110
\end{aligned} \quad (11)$$

In the equation 11, by knowing the contact area, the contact radius can be calculated.

3.2. Cylindrical Contact Mechanics Models

To get a more realistic model, our geometry should approach the geometry of a real sample; therefore, the results can be improved by considering the DNA particles with a cylindrical geometry.

3.2.1. Hertz Contact Theory

By considering a plane stress condition in this problem, the indentation depth and contact radius can be determined as the equations (12-14) [27]:

$$F_{(adh)Hertz}=0 \quad (12)$$

$$\begin{aligned}
\delta_{Hertz}&=\frac{a^2}{2R}\left[2\ln(4R/a)-1\right]\\
&=\frac{F}{L\pi k}\left[\ln(4LR\pi k/F)-1\right]
\end{aligned} \quad (13)$$

$$a_{Hertz}=\frac{4FR}{\pi k} \quad (14)$$

Hertz theory doesn't take the adhesion forces into consideration. In fact, in the presence of surface forces, Hertz contact model loses its effectiveness at small loadings. Thus, in the simulation of nanoparticles manipulation, this theory can be used only when the externally applied force is larger than the surface forces.

3.2.2. JKR Contact Theory

In JKR cylindrical contact model [28], the adhesion forces are considered in the contact region only, and as we move away from the contact zone, the adhesion forces will approach zero. In this model, the relationship between the contact radius and the loading force per unit length is expressed as the equations (15 & 16) [28]:

$$F_{adh}=\frac{\pi k a_{JKR}^2}{4R}-\sqrt{2\pi k a_{JKR}\gamma} \quad (15)$$

$$a_{JkR}=\sqrt[3]{2R^2\gamma/\pi k} \quad (16)$$

Also, the relationship between indentation depth and contact radius can be written as the equation (17) [28]:

$$\delta_{JkR}=\frac{a_{JKR}^2}{R}-\sqrt{\frac{8\pi\gamma a_{JKR}}{3k}} \quad (17)$$

4. SIMULATION AND RESULTS

4.1. Simulation of Spherical Contact

The properties of used materials in the models have been listed in Table 1. The equations used in the simulations are included in the modeling section. The DNA radius in the simulations of contact models is 50 nm. In these simulations, tip radii are 10, 20, and 50 nanometers and have been made from silicon nitride.

Table 1. *DNA and AFM tip properties [29].*

	Elasticity modulus (GPa)	Poisson ratio
DNA	0.1-0.2	0.35-0.5
AFM tip	169	0.27

4.1.1. Simulation of Hertz Spherical Contact

With regards to the dimensions of the considered nanoparticles and the limitation of Hertz model, the simulation was performed up to a maximum indentation depth of 10 nm. The largest magnitude of applied external load is 20 nN. Fig. 2 shows Hertz model for a spherical DNA particle. This figure depicts the contact

region's characteristics in agreement with the theory of Hertz.

In investigating the tip-DNA contact by Hertz contact mechanics model, a simple and ideal case is considered. In this presumption, the surfaces involved in the contact are frictionless and the simulation is based on the behavior of two elastic spheres.

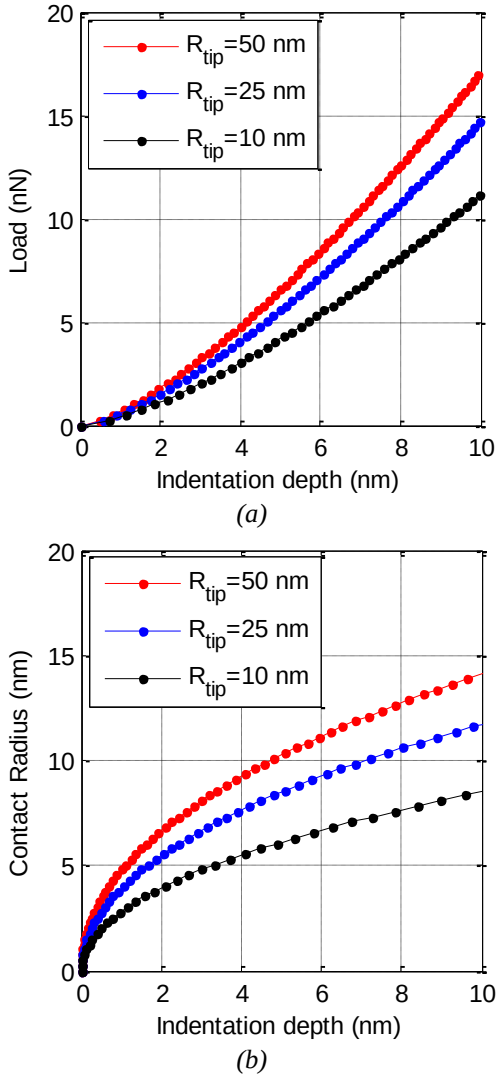

***Figure 2**. Simulation of Hertz contact mechanics model for spherical DNA nanoparticle; (a) Force versus indentation depth, (b) Contact radius versus indentation depth*.

4.1.2. Simulation of JKR Spherical Contact

In the simulation by JKR method, the adhesion force is also taken into consideration. In this simulation method, the existence of the adhesion force causes a change in the geometry of contact when a small external load is exerted. As the contact radius versus indentation depth diagram in Fig. 3 shows, the presence of adhesion at the beginning of contact causes a negative indentation depth in the contact region. The increase of the applied force and, consequently, the indentation depth brings the behavior of this model closer to that of Hertz model.

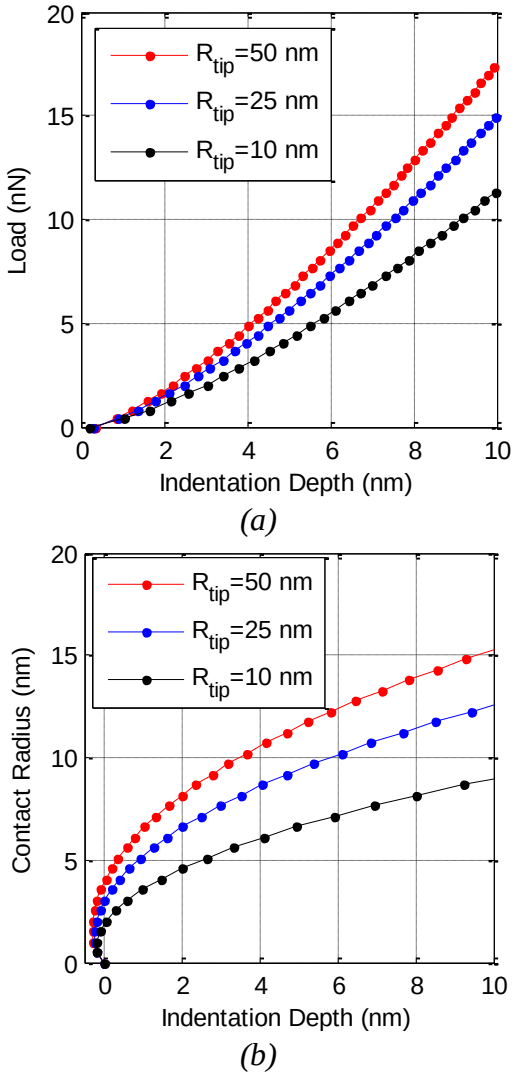

***Figure 3**. Simulation of JKR contact mechanics model for spherical DNA nanoparticle; (a) Force versus indentation depth, (b) Contact radius versus indentation depth*.

4.1.3. Simulation of Chang Spherical Contact

In simulation of the tip-nanoparticle contact by this method, the elastic section in contact was simulated by both the Hertz and Tatara methods. The elastic ranges of contacts in Figs. 4(a) and 4(b) follow the Hertz model, and in Figs. 4(c) and 4(d), they follow the Tatara model. Because the Tatara model has been developed for large deformations, it was also used in the simulations so that the differences of the Chang model with two different elastic regions are determined. The force-displacement and contact radius versus indentation depth curves demonstrate that for the same indentation depth, a smaller applied load is predicted when the elastic region is simulated by Hertz model.

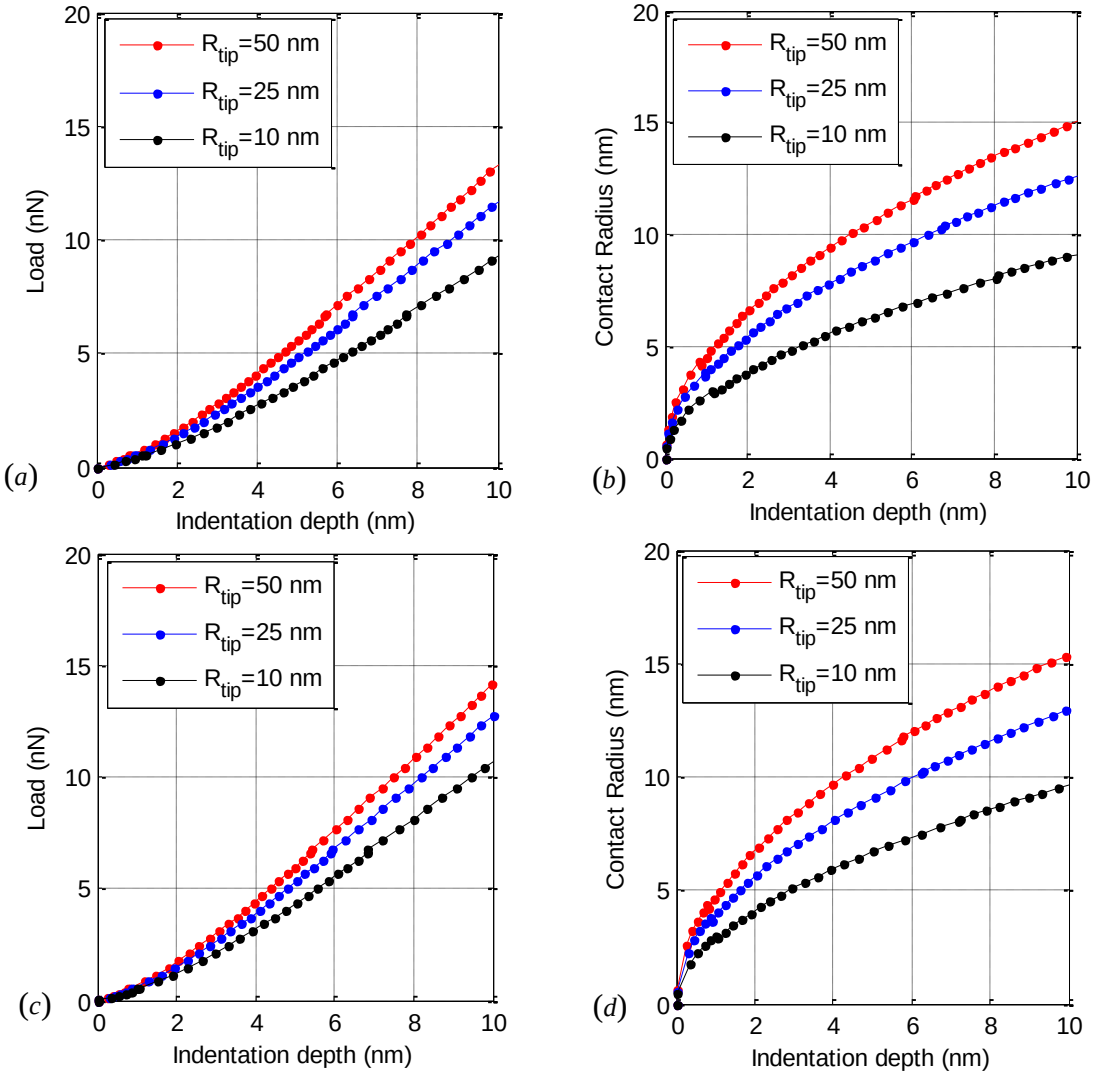

***Figure 4**. Simulation of Chang contact mechanics model for spherical DNA nanoparticle; (a) and (c) Force versus indentation depth, (b) and (d) Contact radius versus indentation depth.*

4.2. Simulation of Cylindrical Contact

In the simulations of cylindrical shapes, due to the geometry of contact, a larger surface is involved in the contact. One of the most effective factors in the contact region is the length of cylinder. Thus, the cylindrical shaped nanoparticle is expected to shows more resistance rather than spherical one against an externally applied force. This resistance includes a smaller contact area and a smaller indentation depth relative to the spherical model, for the same loading. The radius and length of the DNA particle used in the simulation are 50 nm and 200 nm, respectively, also tip radius is 50 nm.

4.2.1. Simulation of Hertz Cylindrical Contact

All the explanations given in the Hertz spherical simulation section are also true, except that the geometry of contact changes. As aforementioned, due to the increase of the contact area, the cylindrical geometry enjoys a higher rigidity relative to the spherical geometry. For the same loading, the indentation depth values diminish relative to the spherical case. This is also confirmed by results.

4.2.2. Simulation of JKR Cylindrical Contact

In the simulation by JKR cylindrical method, the applied properties are similar to the spherical model; and to understand the difference between these two, the loading of both cases is implemented in the same range. Also, the indentation depth diminishes relative to the spherical model and this reduction is more severe compared to that in Hertz model.

4.3. Validation by FEM Simulation

The Finite Element Method was developed due to the need to solve structural analysis and complex elasticity problems. With the advent of finite element software programs, this method has been applied extensively to biological sciences as well. These applications range from the analysis of loads applied on the muscles and organs of the body to the investigation of cells in laboratories and bodies of live organisms. For example, Gladilin et al. investigated the single-axis stretching of cells by employing the 3D finite element analysis method [30]. The study of the Vector finite element modeling of optical tweezers by White showed that this method can be used to estimate the optical trapping efficiency for dielectric objects with undefined shapes [31]. Ladjal et al. modeled the indentation of cells by using a finite element software program and compared their findings with the results of Hertz contact model [32].

4.3.1. Simulation of Spherical Contact by the FEM

The finite element simulation is performed using ABAQUS 6.10-1, Equation solver method is direct and solution technique is full Newton. Due to the high value of the elasticity modulus, the tip was modeled as rigid in the simulation; and in view of the boundary conditions and the manner of loading, the problem was solved by the axial symmetry method and the end of the biological cell is fixed. The materials were considered as elastic. The implemented mesh configuration considered the sensitivity of the contact region. For a more accurate mesh formation, the number of elements in the contact region is higher and the elements are small, and as we move away from the contact region, the elements become larger in dimension. The 525 Quad elements were used for a structured mesh configuration. With regards to the considered assumptions, the schematic of the problem becomes as in Fig. 5. This figure illustrates the geometry of the cell after maximum loading. Maximum indentation depth in this method is 7.99 nm.

Fig. 6 shows the force-indentation depth and contact radius-indentation depth curves for various methods in R_{tip}=50nm. Simulation by the Hertz method is the simplest possible model. The simulation results of Hertz and JKR models in the spherical case are very close to each other, and only because of the presence of the adhesion forces in JKR model, it yields a larger contact radius at identical indentation depths. At low-magnitude forces, for the same value of indentation depth, JKR model yields a larger contact radius relative to Hertz model, because of the adhesion. Because of considering the plastic properties, the elastoplastic models exhibit more flexibility; and for the same applied force, they yield larger indentation depths relative to the elastic models (confirmed by Fig. 6).

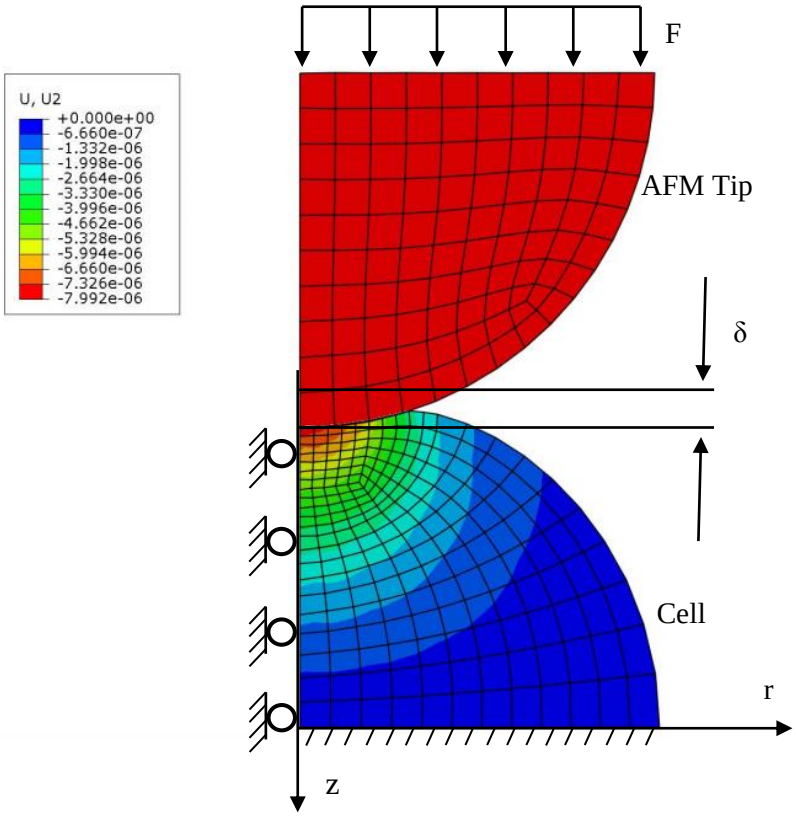

***Figure 5**. Nanoparticle deformation after maximum loading by AFM tip (mm)*

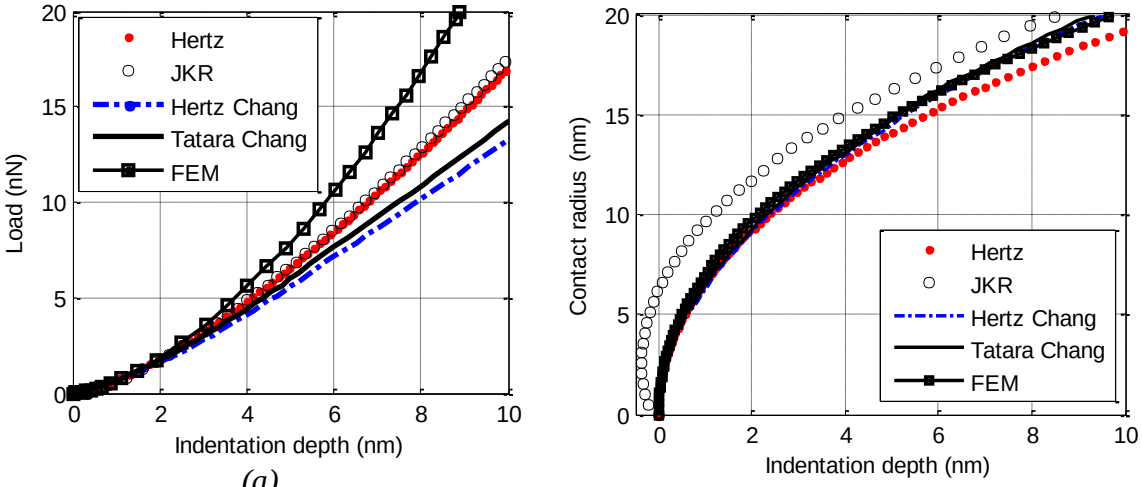

***Figure 6**. Simulation of different contact mechanics models for spherical DNA nanoparticle; (a) Force versus indentation depth, (b) Contact radius versus indentation depth.*

Due to using elastic theories in the elastic range of Chang model, the elastoplastic simulations conform to Hertz and Tatara curves; however, with the rise in the magnitude of the exerted force, they become more distant from the elastic models, which includes both the force-indentation depth and contact radius-indentation depth curves. The simulation by the FEM method shows a higher rigidity compared with the contact theories; and for the same applied load, it reports a smaller indentation depth.

Fig. 7 shows the comparison of contact mechanics models with finite element models when R_{tip}=50nm. Since the behavior of finite element model is limited to elastic area, results of elastoplastic

models should differ much more from finite element results, Fig. 7 confirms this.

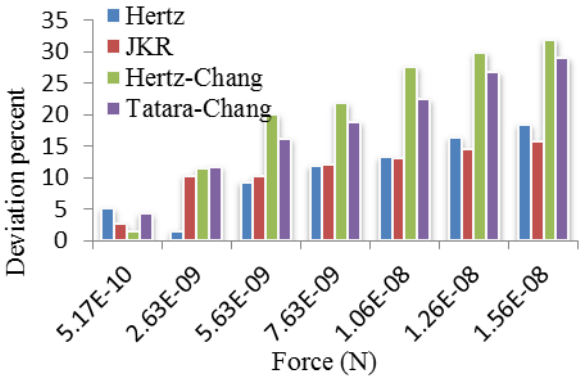

***Figure 7**. Deviation values of FEM versus force in various contact models*.

The elasticity modulus values of biological materials fall in a vast range; which in the simulation by this approach, a constant average value has been considered. This consideration along with the low elasticity modulus values of these particles is the main cause of error generation. If the FEM simulation is performed elastoplastically, the obtained results will be closer to the real values.

4.3.2. Simulation of Cylindrical Contact by FEM

Because of the geometry of the problem here, this problem can no longer be solved two-dimensionally. Thus, the whole geometry has been modeled three-dimensionally. In this simulation, elastic properties have been used to study the behavior of this particle. Similar to the spherical case, the probe tip is considered as a rigid body. Fig. 8 shows an isometric view of the cell after maximum loading. The maximum indentation depth is 2.16 nm in nanoparticle.

After the simulation, the obtained results along with those of Hertz and JKR theories have been presented in Fig. 9. Following the change of geometry from spherical to cylindrical, the JKR model still gives a better prediction of the contact region than the Hertz model.

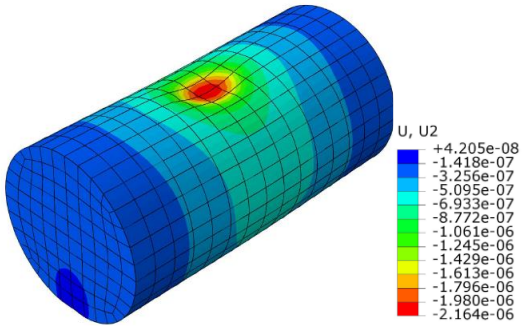

***Figure 8**. Cylindrical nanoparticle deformation after maximum loading (mm)*.

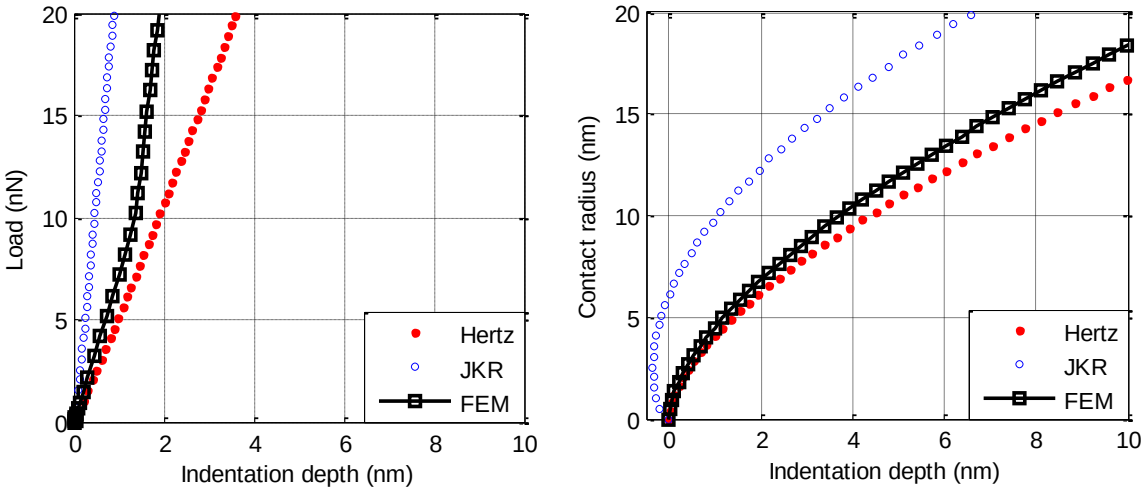

(a) *(b)*

***Figure 9**. Simulation of contact mechanics models for cylindrical DNA nanoparticle; (a) Force versus indentation depth, (b) Contact radius versus indentation depth.*

5. DISCUSSION AND CONCLUSION

Atomic Force Microscope (AFM) is a type of scanning probe microscope which can be used to distinguish material characteristics such as friction, magnetism behaviors and mechanical properties. Also, it can be used for nanoparticle manipulation. The manipulation of biological cells has become of more interest recently; therefore, studying various aspects of this subject can contribute greatly to the progress of this field. One of the relevant and significant aspects in the manipulation of biological cells is the deformation created during the manipulation by the applied forces at the moment of contact.

In order to accurately model bio-particles with complicated shapes, methods such as MD simulation and Monte Carlo can be used. These methods are applicable in small scale physical processes and can be used to extract many physical and thermodynamic properties of the systems under study. One of the problems in using these methods is that they are too time consuming and that currently are limited to systems comprised of only hundreds of atoms. To solve this problem, modeling can be executed in simpler realistic conditions. DNA forms a pack after extraction from cell; spherical geometry has been used in some previews mechanical behavior studies of this bio-particle, using these methods is computationally beneficent [18-20]. In some studies a more accurate structure is used for DNA geometry which consists of a row of connected spheres. There are other models of DNA which suggest cylindrical shape for this nanoparticle, which can be used according to available contact mechanics models [21,22].

This subject is investigated by the contact mechanics models; and in this article, these models and their modified forms for use in biological conditions have been studied. Since the mechanics of contact plays a major role in the manipulation of biological particles, it is necessary to explore and understand its many aspects. There are different models and theories for the identification of the contact region, which describe the contact geometry. The most appropriate model can be selected based on the assumptions of each model and the existing conditions during contact.

One of the innovations of this paper is its unique perspective on the DNA molecule and the describing of various contact theories including the elastoplastic contact model for this nanoparticle. The other contribution is the use of finite element method in micro and nano scales to investigate the behavior of DNA, which can be very useful in extending and developing the FEM techniques for analytical problems which are complex and hard to solve. With the increase of computational capacities, which is required by the finite element method, there can be optimism in the future of FEM-based research activities.

Simulation by the Hertz method is the simplest possible model. The simulation results of Hertz and JKR models in the spherical case are very close to each other, and only because of the presence of the adhesion forces in JKR model, it yields a larger contact radius at identical indentation depths. Also, in the elastoplastic theories, due to the consideration of plastic contact, the results deviate from those of the Hertz model (as an elastic model) as the applied force increases in magnitude. The elastic simulation of DNA was performed by Hertz and JKR models in the cylindrical case and the results of the finite element method were also presented along with these two simulations for comparison. Considering the fact that JKR model includes adhesion effects and that adhesion effects have great impact on bio-particles, it is recommended that the contact model is selected according to the material of the target particle. JKR model is suitable for cases that have a considerable adhesion. Because of the contact geometry, cylindrical contact exhibits a higher

resistance relative to spherical contact model and indicates smaller indentation depth and contact radius at the same loading. This is also verified by the FEM results. The impact of tip radius was also studied in this paper, it was observed that due to force distribution, as the tip radius decreases, the indentation depth increases and the contact radius decreases.

One of the sources of error in FEM simulations is the assumption of elastic contact between two bodies during impact. In addition to the mentioned source of error, the truncation error and the simplification of the physical model can also be cited for the FE model. Of course, one should not forget the low elasticity modulus of the DNA particle, because it causes severe length deformations. The variety of the elasticity modulus values is another cause of error. The most difference values of indentation depth in finite element simulation results in spherical contact mode with Hertz, JKR, Hertz-Chang, and Tatara-Chang models are 18.5%, 15.9%, 32.0%, and 29.0% respectively. This shows that the difference is considerable and cannot be ignored.

REFERENCES

1. Wu, A., Yu, L., Li, Z., Yang, H., Wang, E. (2004). "Atomic force microscope investigation of large-circle DNA molecules", *Analytical biochemistry*, 325(2): 293-300.
2. Sitti, M. (2001). "Survey of nanomanipulation systems", *In: Nanotechnology, 2001. IEEE-NANO 2001. Proceedings of the 2001 1st IEEE Conference on*, 75-80.
3. Tafazzoli, A., Sitti, M. (2004). "Dynamic modes of nanoparticle motion during nanoprobe-based manipulation", *In: Nanotechnology, 2004. 4th IEEE Conference on*, 35-37.
4. Korayem, M. H., Taheri, M., Zakeri, M. (2012). "Sensitivity analysis of nanoparticles manipulation based on different friction models", *Applied Surface Science*, 258 (18): 6713-6722.
5. Korayem, M. H., Rastegar, Z., Taheri, M. (2012). "Application of Johnson–Kendall–Roberts model in nanomanipulation of biological cell: air and liquid environment", *Micro & Nano Letters*, 7(6): 576-580.
6. Korayem, M. H., Khaksar, H., Taheri, M., (2015). "Effective Parameters in Contact Mechanic for Micro/nano Particle Manipulation Based on Atomic Force Microscopy", *International Journal of Nanoscience and Nanotechnology*, 11(2): 83-92.
7. Korayem, M. H., Hefzabad, R. N., Homayooni, A., Aslani, H. (2016). "Molecular dynamics simulation of nanomanipulation based on AFM in liquid ambient", *Applied Physics A*, 122 (11): 977-986.
8. Firouzi, M., Nejat Pishkenari, H., Mahboobi, S., Meghdari, A. (2014). "Manipulation of biomolecules: A molecular dynamics study", *Current Applied Physics*, 14(9): 1216-1227.
9. Korayem, M. H., (2016). "Sensitivity Analysis of the Critical Conditions of AFM-Based Biomanipulation of Cylindrical Biological Particles in Various Biological Mediums by Means of the Sobol Method", *International Journal of Nanoscience and Nanotechnology*, 12(3): 149-166.
10. Dimitriadis, E. K., Horkay, F., Maresca, J., Kachar, B., Chadwick, R. S., (2002). "Determination of elastic moduli of thin layers of soft material using the atomic force microscope", *Biophysical journal*, 82 (5): 2798-2810.
11. Alonso J. L., Goldmann W. H. (2003). "Feeling the forces: atomic force microscopy in cell biology", *Life sciences*, 72(23): 2553-2560.
12. Briscoe, B., Sebastian, K., Adams, M. (1994). "The effect of indenter geometry on the elastic response to indentation", *Journal of Physics D: Applied Physics*, 27(6): 1156.
13. Bolduc, J-F., Lewis, L. J., Aubin C-É., Geitmann, A. (2006). "Finite-element analysis of geometrical factors in micro-indentation of pollen tubes", *Biomechanics and modeling in mechanobiology*, 5 (4): 227-236.
14. Gibbons, M. M., Klug, W. S. (2007). "Nonlinear finite-element analysis of nanoindentation of viral capsids", *Physical Review E*, 75(3): 031901.
15. Korayem, M. H., Hefzabad, R. N., Taheri M, Mahmoodi, Z. (2014). "Finite Element Simulation of Contact Mechanics of Cancer Cells in Manipulation Based on Atomic Force Microscopy", *International Journal of Nanoscience and Nanotechnology*, 10(1): 1-12.
16. Korayem, M. H., Rastegar, Z. (2012). "Application of Nano-Contact Mechanics Models in Manipulation of Biological Nano-Particle: FE Simulation", I*nternational Journal of Nanoscience and Nanotechnology*, 8(1): 35-50.
17. Egli, M., Saenger, W. (2013). "*Principles of nucleic acid structure*", Springer Science & Business Media.
18. Arsuaga, J., Tan, RK-Z., Vazquez, M., Sumners, D. W., Harvey, S. C. (2002) "Investigation of viral DNA packaging using molecular mechanics models", *Biophysical chemistry*, 101: 475-484.

19. Comolli, L. R., Spakowitz, A. J., Siegerist, C. E., Jardine, P. J, Grimes, S., Anderson, D. L., Bustamante, C., Downing, K. H. (2008). "Three-dimensional architecture of the bacteriophage φ29 packaged genome and elucidation of its packaging process", *Virology*, 371(2): 267-277.
20. LaMarque J. C., Le T. V. L., Harvey S. C. (2004). "Packaging double- helical DNA into viral capsids", *Biopolymers*, 73(3): 348-355.
21. Purohit, P. K., Kondev, J., Phillips, R. (2003). "Mechanics of DNA packaging in viruses", *Proceedings of the National Academy of Sciences*, 100(6): 3173-3178.
22. Purohit P. K., Kondev, J., Phillips, R. (2003). "Force steps during viral DNA packaging?", *Journal of the Mechanics and Physics of Solids*, 51(11): 2239-2257.
23. Purohit, P.K., Inamdar, M. M., Grayson, P.D., Squires, T. M., Kondev, J., Phillips, R. (2005). "Forces during bacteriophage DNA packaging and ejection", *Biophysical journal*, 88 (2): 851-866.
24. Hertz H (1896) Über die Berührung Fester Elastischer Körper (on the Contact of Elastic Solids). J. Reineund Angewandte Mathematik 92 (1881) 156. Miscellaneous Papers by H Hertz, Macmillan, London
25. Johnson, K., Kendall, K., Roberts, A. (1971) "Surface energy and the contact of elastic solids", *Proceedings of the royal society of London A mathematical and physical sciences*, 324 (1558): 301-313.
26. Zhao, J., Nagao, S., Zhang, Z. (2012) "Loading and unloading of a spherical contact: From elastic to elastic–perfectly plastic materials", *International Journal of Mechanical Sciences*, 56 (1): 70-76.
27. Johnson, K.L., Johnson, K.L. (1987). " *Contact mechanics*", Cambridge university press.
28. Chen, S., Wang, T., (2006). "General solution to two-dimensional nonslipping JKR model with a pulling force in an arbitrary direction", *Journal of colloid and interface science*, 302 (1): 363-369.
29. Legay, G., Finot, E., Meunier-Prest, R., Cherkaoui-Malki, M., Latruffe, N., Dereux, A. (2005). "DNA nanofilm thickness measurement on microarray in air and in liquid using an atomic force microscope", *Biosensors and Bioelectronics*, 21 (4): 627-636.
30. Gladilin, E., Micoulet, A., Hosseini, B., Rohr, K., Spatz, J., Eils, R. (2007). "3D finite element analysis of uniaxial cell stretching: from image to insight", *Physical biology*, 4(2): 104.
31. White, D. A. (2000) "Vector finite element modeling of optical tweezers", *Computer physics communications*, 128(3): 558-564.
32. Ladjal, H., Hanus, J-L., Pillarisetti, A., Keefer, C., Ferreira, A., Desai, J. P., (2012) "Reality-based real-time cell indentation simulator", *Mechatronics, IEEE/ASME Transactions on*, 17(2): 239-250.